Reinvestigation of the decay properties of ^{261,262}Bh at the gas-filled recoil separator SHANS2

Z. Zhao,[1,2] Z. G. Gan,[1,2,3,*] Z. Y. Zhang,[1,2] J. G. Wang,[1] M. H. Huang,[1,2] L. Ma,[1] H. B. Yang,[1] M. M. Zhang,[1] C. L. Yang,[1] S. Y. Xu,[1,2] X. Y. Huang,[1,2] Z. C. Li,[1,2] L. C. Sun,[1,4] X. L. Wu,[1] Y. S. Wang,[1] Y. L. Tian,[1] Y. H. Qiang,[1] J. Y. Wang,[1] W. X. Huang,[1] Y. He,[1] L. T. Sun,[1] V. K. Utyonkov,[5] A. A. Voinov,[5] Yu. S. Tsyganov,[5] and A. N. Polyakov[5]

[1]*Institute of Modern Physics, Chinese Academy of Sciences, Lanzhou 730000, China*

[2]*School of Nuclear Science and Technology, University of Chinese Academy of Sciences, Beijing 100049, China*

[3]*Advanced Energy Science and Technology Guangdong Laboratory, Huizhou 516000, China*

[4]*Department of Physics, Guangxi Normal University, Guilin 541004, China*

[5]*Joint Institute for Nuclear Research, RU-141980 Dubna, Russian Federation*

(Received 24 October 2023; accepted 21 February 2024; published 20 March 2024)

The isotopes ^{261,262}Bh were reinvestigated by using the cold fusion reaction ^{54}Cr + ^{209}Bi. The evaporation residues were separated by the gas-filled recoil separator SHANS2 (Spectrometer for Heavy Atoms and Nuclear Structure-2) and identified by means of the recoil-α-correlation method. The α-decay properties of ^{261,262}Bh were measured and the results are consistent with the previously reported values. Based on the measured half-lives, the existence of two distinct states of ^{262}Bh was confirmed, whereas ^{261}Bh lacked any isomer with α-decay properties. Two spontaneous fission events potentially from ^{262}Bh and/or ^{261}Bh were detected and the production cross sections at beam energies of 264.1 and 270.4 MeV were obtained.

DOI: 10.1103/PhysRevC.109.034314

I. INTRODUCTION

Alpha-decay spectroscopy has been recognized as a powerful technique for the identification of superheavy nuclei and the study of their decay properties [1]. The macroscopic model predicts that nuclei with $Z \gtrsim 100$ are unstable due to spontaneous fission (SF) [2]. Owing to the pivotal role of the shell effect [3], over 100 superheavy nuclei ($Z \geqslant 104$) have been synthesized to date. The presence of shell effect leads to the suppression of SF, while α decay emerges as a notable mode.

Cold fusion reaction, which utilizes medium-mass nuclei as the projectiles and ^{208}Pb or ^{209}Bi as the targets, is one of the most important methods for synthesizing superheavy elements and investigating their decay properties. Oganessian *et al.* [4] first studied the SF products in ^{54}Cr + ^{209}Bi and ^{55}Mn + ^{208}Pb cold fusion reactions. In 1981, element 107 was identified for the first time through α-correlation chains by Münzenberg *et al.* [5] via the ^{209}Bi(^{54}Cr, 1n) ^{262}Bh reaction. This result was confirmed by the subsequent independent experiments with the same projectile-target combination by the same group [6]. In 1997, the element received its official name “bohrium” [7].

The chemical properties of element 107 and the decay properties of its isotopes have been extensively investigated. In 2000, ^{267}Bh was produced by Eichler *et al.* [8] via the fusion evaporation reaction ^{249}Bk(^{22}Ne, 4n), and the adsorption enthalpy of BhO_3Cl was measured as $\Delta H_{\rm ads} = -75^{+9}_{-6}$ kJ/mol using isothermal gas chromatography. Their research demonstrates that Bh exhibits typical characteristics of the Group VII elements, despite the influence of relativistic effects on its chemical properties. Up to now, 11 isotopes of Bh have been identified [3,5,9–15].

The early studies of ^{261,262}Bh [5,6] revealed that ^{262}Bh exhibits two distinct states. Ten α-decay events assigned to ^{261}Bh were observed with a half-life of $11.8^{+5.3}_{-2.8}$ ms. In 2006, Folden, III, *et al.* [16] reported the two isotopes produced by the ^{55}Mn + ^{208}Pb reaction. Their results confirmed the observations of Refs. [5,6]. The ^{209}Bi(^{54}Cr, 1n) ^{262}Bh reaction was also investigated by Štreicher *et al.* [17], the yield of ^{262}Bh was increased several times compared to the previous experiments, and the existence of two states of ^{262}Bh was also verified. In 2008, Nelson *et al.* [18] reported experimental results from both reactions. An excitation function for the production of ^{262}Bh via the ^{54}Cr + ^{209}Bi reaction was measured, which generally agreed with the previous works [5,6]. Later on, more detailed decay properties of ^{261,262}Bh were investigated by Heßberger *et al.* [10,19].

To study superheavy nuclei and elements with extremely low production cross sections, the superconducting linear accelerator CAFE2 (China Accelerator Facility for Superheavy Elements) was constructed and the new gas-filled recoil separator SHANS2 [20,21] was developed at the Institute of Modern Physics, Chinese Academy of Sciences, in 2019. A series of experiments was performed at the separator with beams of ^{54}Cr, ^{40}Ar, and ^{48}Ca. In this paper, we report the results of ^{261,262}Bh produced in the reactions ^{209}Bi(^{54}Cr, 1-2n) ^{261,262}Bh.

*Corresponding author: zggan@impcas.ac.cn

II. EXPERIMENT

The experiment was performed at the SHANS2 separator with CAFE2. The beam of $^{54}Cr^{17+}$ was produced by an electron cyclotron resonance ion source and accelerated to 264.1 and 270.4 MeV, which were chosen for the observations of ^{262}Bh and ^{261}Bh, respectively. The average beam intensity was about 315 pnA. The ^{209}Bi target material with a thickness of 500 $\mu g/cm^2$ was evaporated on a 60-$\mu g/cm^2$-thick carbon layer. Twenty targets were mounted on a rotating wheel with a diameter of 50 cm.

The recoiled evaporation residues (ERs) of interest were separated in-flight from the primary beam particles and other unwanted reaction products using the SHANS2 separator. The separator was filled with pure helium gas at a pressure of 1 mbar, and the ERs underwent charge equilibrium through collisions with gas molecules. The magnetic rigidity of 1.8–2.1 Tm was set to transmit ERs to the focal plane, where the ERs were implanted into a 300-μm-thick double-sided silicon strip detector (DSSD). The DSSD had an active area of 128×48 mm^2 with 128 vertical strips on the back side and 48 horizontal ones on the front side, and it was used to determine the vertical and horizontal positions of the implanted particles. In the offline data analysis, ERs were identified based on the position on the DSSD as well as on energy and time information obtained from successive α decays, in which the emitted α particles were denoted as $\alpha 1$, $\alpha 2$, and so on. To detect α particles escaping from the DSSD, six side silicon detectors (SSD) with an active area of 120×63 cm^2 and a thickness of 500 μm were strategically positioned around the DSSD. The detection efficiency of α particles was approximately 87(6)%, which was measured in the test reaction ^{48}Ca + ^{208}Pb.

To detect prompt or delayed γ rays, a Clover detector consisting of four Ge crystals, each of 60 mm in diameter and 90 mm in length, and a HPGe detector with a relative efficiency of 70% were mounted behind the DSSD and on a side of the SSD, respectively. Energy calibration of the detectors was performed using ^{133}Ba and ^{152}Eu. The energy resolutions (full width at half maximum) were 3.8 and 9.6 keV, respectively, at the 122-keV peak of the ^{152}Eu source.

V1724 wave-form digitizers with a 100-MHz sampling from CAEN S.p.A [22] were used for data acquisition. The wave forms from the charge-sensitive preamplifier were recorded in 20-μs-long traces for the signals from the front of the DSSD and in 30-μs-long traces from the back. The silicon detectors were calibrated by using a standard ^{239}Pu - ^{241}Am - ^{244}Cm hybrid α source and known α-decay peaks from the ^{54}Cr + ^{159}Tb reaction. The energy resolutions were about 30 keV for full-energy α events detected by the DSSD and 90 keV for reconstructed events detected by the DSSD and SSDs.

III. RESULTS AND DISCUSSION

The α-decay energies and half-lives of ^{262}Bh and ^{261}Bh and their daughter nuclei are similar; thus, the assignment has to rely on their granddaughters ^{254}Lr and ^{253}Lr. The data analysis revealed that electron capture (EC) is a significant decay mode in the correlation chains of ^{262}Bh. Due to the presence of an EC-α branch and an EC branch in ^{258}Db and ^{254}Lr, the isotope ^{254}No was generated. Therefore, ^{262}Bh was identified by the α-particle energies and lifetimes of the granddaughter ^{254}Lr and the great-granddaughter ^{254}No. At the beam energy of 264.1 MeV, 137 correlation chains were assigned to ^{262}Bh, while ^{261}Bh was absent. At 270.4 MeV, 6 events from ^{262}Bh and 26 events from ^{261}Bh were detected, respectively. The numbers of observed ^{261,262}Bh at two beam energies are listed in Table I.

TABLE I. The numbers of observed ^{262}Bh and ^{261}Bh at two beam energies.

Isotopes	E_{beam} = 264.1 MeV	E_{beam} = 270.4 MeV
^{262}Bh	137	6
^{261}Bh	0	26

A. ^{262}Bh

A total of 143 α-decay events of ^{262}Bh were observed in this work. Figure 1(a) shows the energy spectrum of 81 full-energy events. The broad distribution suggests the possible existence of an isomeric state, as well as energy summing effects resulting from the internal conversion electrons and α particles. The prior research [19] indicated that the identification of ground and isomeric states in ^{262}Bh remains uncertain. Unfortunately, our research has not yielded any further insights into this issue. Therefore, a definitive differentiation

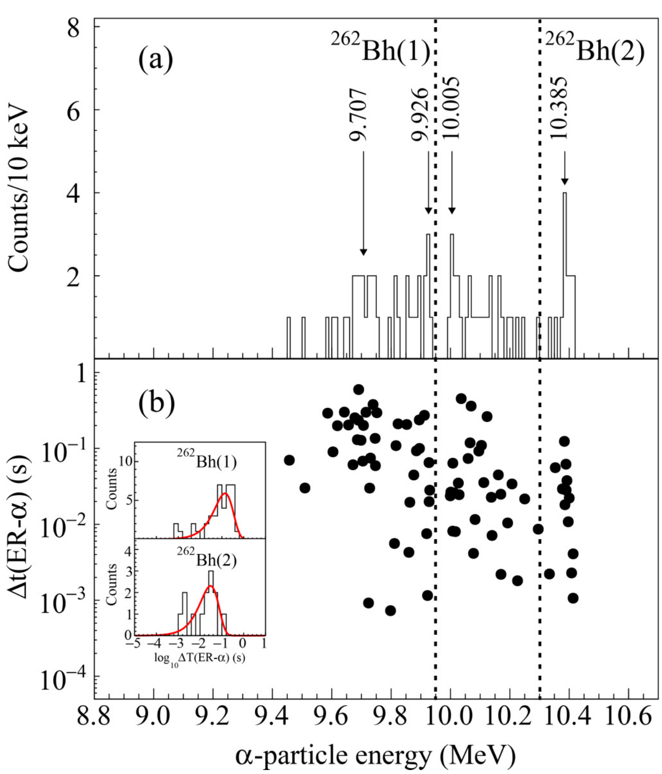

FIG. 1. (a) α-decay spectrum of ^{262}Bh for full-energy events on the DSSD. (b) Two-dimensional scatter plot of lifetime versus energy of α decays of ^{262}Bh. Histograms depicting the distribution of lifetimes for ^{262}Bh(1) and ^{262}Bh(2) are presented in the inset graph, where the red curves are the fitted decay-time distributions.

TABLE II. Summary of the half-lives for ^{262}Bh(1) and ^{262}Bh(2).

^{262}Bh(1)	^{262}Bh(2)	Ref.
96^{+18}_{-13} ms	21^{+8}_{-5} ms	This work
115^{+231}_{-75} ms	$4.7^{+2.3}_{-1.6}$ ms	[5]
102 ± 26 ms	8.0 ± 2.1 ms	[6]
135^{+15}_{-12} ms	$13.2^{+1.2}_{-1.0}$ ms	[17]
120^{+55}_{-29} ms	16^{+14}_{-5} ms	[18]
83 ± 14 ms	22 ± 4 ms	[19]

between ground and isomeric states cannot be established. However, despite the lack of a comprehensive understanding of their differences, we can still utilize the notations (1) and (2) to describe the long-lived and short-lived states of ^{262}Bh for our ongoing research.

Figure 1(b) is partitioned into three intervals based on the α-particle energies of 9.95 and 10.3 MeV. The energy intervals below 9.95 MeV and above 10.3 MeV are assigned to ^{262}Bh(1) and ^{262}Bh(2), respectively. Due to the intricate nuclear structure of ^{258}Db, distinguishing between ^{262}Bh(1) and ^{262}Bh(2) within the energy interval of 9.95 to 10.3 MeV poses a significant challenge. Therefore, the half-lives of ^{262}Bh(1) and ^{262}Bh(2) are deduced without considering the events within this interval. The half-lives of ^{262}Bh(1) and ^{262}Bh(2) are determined to be 96^{+18}_{-13} and 21^{+8}_{-5} ms, respectively. Table II summarizes the half-lives obtained from this work and all the previously reported values for both states of ^{262}Bh. The half-lives are in agreement with the results of Nelson *et al.* [18] and Heßberger *et al.* [19], although there are differences in the division of ^{262}Bh(1) and ^{262}Bh(2) based on the α-particle energy. The distinction between ^{262}Bh(1) and ^{262}Bh(2) is somewhat ambiguous and requires further investigation with higher statistics.

Figure 2 shows a two-dimensional scatter plot of the α-γ prompt coincidence from ^{262}Bh and the corresponding γ spectrum. The energies of 129, 138, and 155 keV were found to be consistent with those reported in previous literature [19]. The 129- and 138-keV events are interpreted as the $K_{\alpha 2}$ and $K_{\alpha 1}$ lines from ^{258}Db, respectively. The 155-keV line is more similar to an $E1$ transition. Unfortunately, the 61-keV event cannot be assigned definitely in this work.

Figure 3 shows the ER-α1-α2 correlation of α decays between the parent ^{262}Bh and the daughter ^{258}Db. Only those events detected with full energy by the DSSD at the beam energy of 264.1 MeV are included. The searching time window is 1 s for the ER-α1 pair and 30 s for the α1-α2 pair. The α-decay energies of ^{258}Db are mainly in the range from 8.9 to 9.3 MeV, which is consistent with the results in Refs. [19,23]. The half-lives of ^{258}Db following decays of ^{262}Bh(1) and ^{262}Bh(2) are determined to be $4.0^{+1.1}_{-0.7}$ s and $3.0^{+1.8}_{-0.8}$ s, respectively. The former might be regarded as decay from the long-lived (4.41 ± 0.21 s [23]) isomer in ^{258}Db and the latter is tentatively assigned to decay from the short-lived (2.17 ± 0.36 s [23]) ground state in ^{258}Db.

The α-decay half-life of the granddaughter ^{254}Lr was determined to be 15 ± 2 s, which is consistent with the literature value of 18.1 ± 1.8 s [24]. Utilizing the α-particle energy of

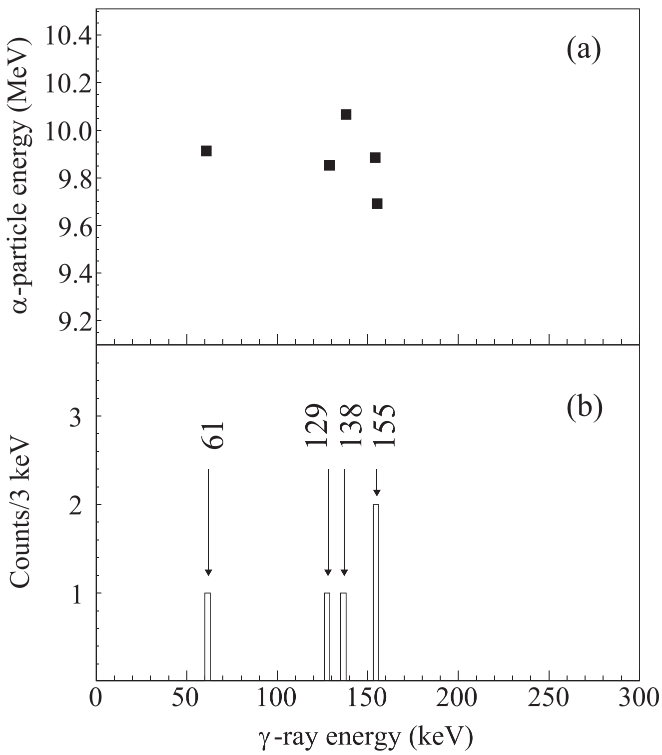

FIG. 2. (a) Two-dimensional scatter plot of α-γ prompt coincidence from ^{262}Bh. (b) The γ spectrum from the α-γ prompt coincidence events.

^{258}Rf [25] and ^{254}No [26], two full-energy events, which are assigned to the decay chains of the types ER(^{262}Bh) $\xrightarrow{\alpha}$ ^{258}Db $\xrightarrow{EC}$ ^{258}Rf $\xrightarrow{\alpha}$ ^{254}No and/or ER(^{262}Bh)$\xrightarrow{\alpha}$^{258}Db $\xrightarrow{\alpha}$ ^{254}Lr $\xrightarrow{EC}$ ^{254}No, were observed.

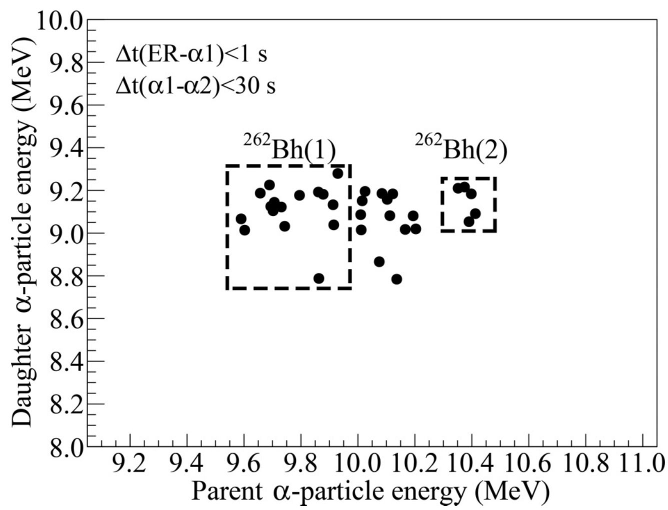

FIG. 3. Two-dimensional scatter plot of α-particle energies from the parent ^{262}Bh and the daughter ^{258}Db for the ER-α1-α2 correlation. The searching time window is 1 s for the ER-α1 pair and 30 s for the α1-α2 pair. Only those events detected with full energy by the DSSD at the beam energy of 264.1 MeV are included.

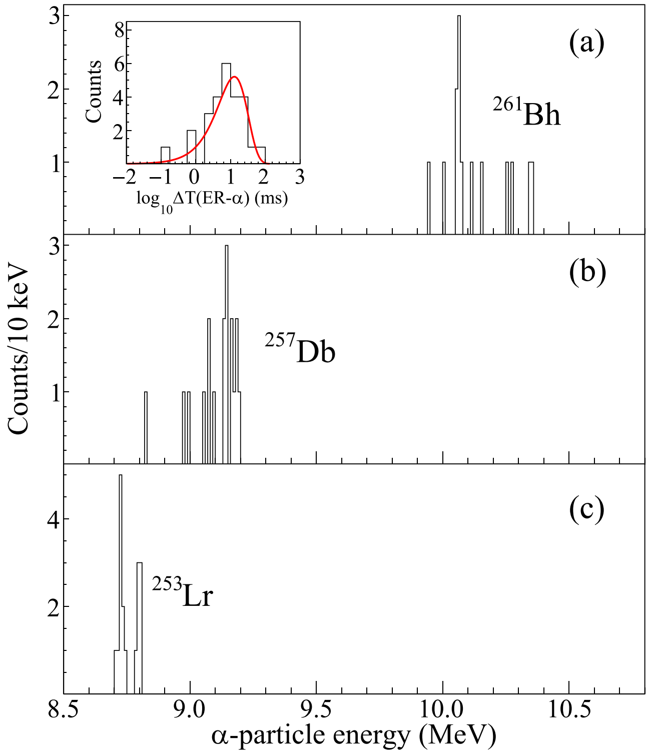

FIG. 4. The α-decay energy spectra of ^{261}Bh, ^{257}Db, and ^{253}Lr. The lifetime distribution of ^{261}Bh is presented in the inset graph; the red curve shows the calculated decay-time distribution with a half-life of 8.9 ms.

At the beam energy of 270.4 MeV, we observed an ER(^{262}Bh) $\xrightarrow{\alpha}$ ^{258}Db $\xrightarrow{EC}$ ^{258}Rf $\xrightarrow{SF}$ correlation chain. It was assigned to ^{262}Bh(1) based on the lifetime of 206 ms and the α-particle energy of 9.855 MeV of the ER. At 264.1 MeV, 25 correlation chains mentioned above were assigned to ^{262}Bh.

The production cross section of ^{262}Bh was determined to be 703^{+261}_{-246} pb at the beam energy of 264.1 MeV and 56^{+76}_{-40} pb at 270.4 MeV. The transmission efficiency of the SHANS2 separator for cross-section calculations was measured to be 56(10)% through the ^{208}Pb(^{48}Ca, $2n$) ^{254}No reaction.

B. ^{261}Bh

A total of 26 correlation chains of ^{261}Bh were observed, 3 of which have the chain of ER(^{261}Bh) $\xrightarrow{\alpha}$ ^{257}Db $\xrightarrow{\alpha}$ ^{253}Lr $\xrightarrow{SF}$. The half-life of ^{261}Bh was determined to be $8.9^{+2.2}_{-1.5}$ ms, which corresponds to the published values of $11.8^{+5.3}_{-2.8}$ ms [6], 10^{+14}_{-5} ms [16], and $6.7^{+3.8}_{-1.8}$ ms [18]. Figure 4 shows the α-particle energy spectra of the parent ^{261}Bh, the daughter ^{257}Db, and the granddaughter ^{253}Lr.

The energy spectrum of ^{261}Bh shows a wide distribution as a result of energy summing effects caused by internal conversion electrons and α particles. An obvious peak is observed at 10.061 MeV in the energy spectrum of ^{261}Bh. It is attributed to the α decay originating from the $5/2^{-}[512]$ state of the parent to the $5/2^{-}[512]$ state of the daughter and piles up with the internal conversion electron from the $5/2^{-}[512]$ to the $1/2^{-}[521]$ proton single-particle state of the daughter [10]. The energies and half-lives of α decays for the parent, daughter, and granddaughter nuclei of ^{261}Bh from this work and the literature are summarized in Table III.

A γ event was detected in the α-γ prompt coincidence, with a corresponding γ energy of 245 keV detected by the Clover detector. This event is assigned to ^{261}Bh based on the α-decay energy of the granddaughter ^{253}Lr. The γ event of ^{257}Db might be interpreted as an $E1$ transition from the $7/2^{-}[514]$ to the $9/2^{+}[624]$ proton single-particle state, based on the previously suggested decay scheme in Ref. [10].

In this work, we observed 17 full-energy events of ^{253}Lr on the DSSD. By considering a detection efficiency of 55% for events with full energy deposited in DSSD, 31 α-decay events in total from ^{253}Lr were expected, of which 18 events were originated from ^{253}Lr(1) and 13 from ^{253}Lr(2). Three ER(^{261}Bh) $\xrightarrow{\alpha}$ ^{257}Db $\xrightarrow{\alpha}$ ^{253}Lr $\xrightarrow{SF}$ correlation chains were observed at the beam energy of 270.4 MeV. If the three events were assigned to ^{253}Lr(1), the spontaneous fission branching ratio of ^{253}Lr(1) would be deduced as 14^{+10}_{-8}%, which is slightly larger than the reported value 8(5)% in Ref. [27]. This may potentially be attributed to a statistical error, wherein an increase in the count leads to a corresponding improvement in the accuracy of the branching ratio.

TABLE III. α-particle energies and half-lives of ^{261}Bh, the daughter ^{257}Db, and the granddaughter ^{253}Lr from this work and the literature.

	This work			Literature data		
Isotope	E_α/keV	Number	$T_{1/2}$	E_α/keV	$T_{1/2}$	Ref.
^{261}Bh	≈10 000	22[a]	$9.0^{+2.4}_{-1.6}$ ms	≈10 000	$11.8^{+3.9}_{-2.4}$ ms	[10]
	9900-10 160	13[a]	$8.4^{+3.2}_{-1.8}$ ms	9900–10 160	$11.5^{+7.0}_{-3.2}$ ms	[10]
	10 160–10 400	9[a]	$9.8^{+4.9}_{-2.5}$ ms	10 160–10 400	$12.0^{+6.0}_{-3.0}$ ms	[10]
^{257}Db(1)	9161 ± 13	11	$0.48^{+0.21}_{-0.11}$ s	9163 ± 10	$0.76^{+0.15}_{-0.11}$ s	[27]
^{257}Db(2)	9075 ± 13	4	$0.91^{+0.63}_{-0.26}$ s	9074 ± 10	$1.50^{+0.19}_{-0.15}$ s	[27]
	8987 ± 13	2		8967 ± 15		[27]
^{253}Lr(1)	8725 ± 13	10	$1.23^{+0.57}_{-0.29}$ s	8722 ± 10	$1.49^{+0.30}_{-0.21}$ s	[27]
^{253}Lr(2)	8797 ± 13	7	$0.70^{+0.42}_{-0.19}$ s	8794 ± 10	$0.57^{+0.07}_{-0.06}$ s	[27]

[a]Full-energy and reconstructed events.

The production cross section of ^{261}Bh was determined to be 174^{+92}_{-77} pb at the beam energy of 270.4 MeV, while no ^{261}Bh was observed at 264.1 MeV, thus only an upper limit of 33 pb can be estimated.

C. Spontaneous fission

We scrutinized all the data to determine whether any SF events could be attributed to ^{262}Bh or ^{261}Bh and found two such ER-SF events, which correspond to the excitation energies of the compound nucleus at 17.0 and 22.0 MeV, respectively. The first ER-SF event at the beam energy of 264.1 MeV shows an implantation energy of 14.7 MeV, with a position at the strip number 107 in the horizontal direction and 29 in the vertical direction, followed by a signal of 174.2 MeV after 336.6 ms. The lifetime of the ER significantly exceeds the half-life of ^{262}Bh(2) or ^{261}Bh; thus, it may be attributed to either ^{262}Bh(1) or its EC-decay product ^{262}Sg. However, the absence of a detectable second fission fragment in this event presents challenges in distinguishing them from projectilelike particle signals. The second ER-SF event at the incident energy of 270.4 MeV was implanted in the DSSD with an ER energy of 15.5 MeV, with a position at the strip number 75 in the horizontal direction and 26 in the vertical direction. A signal from a second fission fragment was detected by the SSD, resulting in a total SF energy of 179.9 + 8.3 MeV and a lifetime of 18.2 ms. However, determining whether the ER is ^{262}Bh or ^{261}Bh based on its lifetime presents a challenging task.

D. Excitation function

The excitation functions of ^{262}Bh and ^{261}Bh in the ^{54}Cr + ^{209}Bi reaction system are shown in Fig. 5, where the theoretical values are calculated from the HIVAP code [28,29], and the experimental data are obtained from this work and Refs. [5,6,18]. In the HIVAP code, the BARFAC parameter is used to adjust the fission barrier height of the liquid-drop model, thereby regulating the competition between fission and alternative decay channels, such as light particle evaporation and γ-ray emission. Nevertheless, the liquid-drop model predicts an almost negligible fission barrier in the region of superheavy nuclei and adjusting the BARFAC parameter does not effectively modify the height of the fission barrier. The HIVAP code takes into account the extra-push mechanism to increase the height of the interaction barrier, consequently suppressing fusion probability. The curves in Fig. 5 were generated by adjusting the extra-push parameters within the HIVAP code framework.

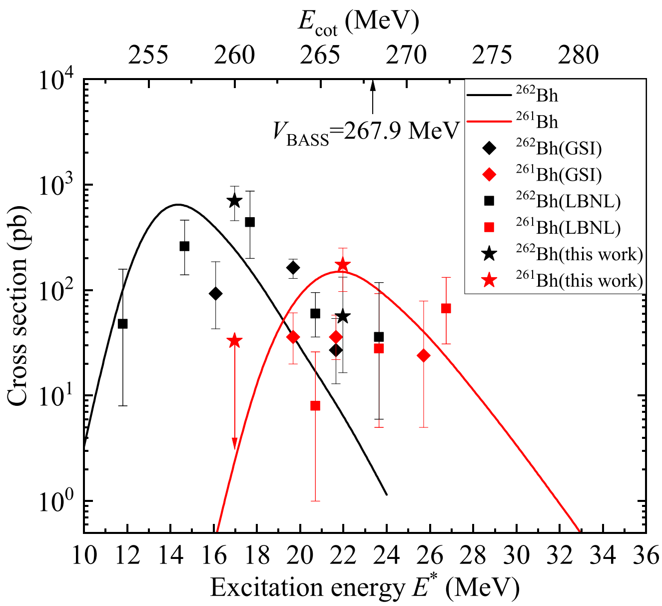

FIG. 5. The excitation functions of ^{262}Bh and ^{261}Bh. E_{cot} represents the beam energy of ^{54}Cr at the center of target in the laboratory system. The theoretical curves were calculated by using the HIVAP code and the points are experimental data from GSI [5,6], LBNL [18], and this work. The masses of ^{54}Cr, ^{209}Bi, and the compound nuclei ^{263}Bh are taken from AME2020 [30]. The Coulomb barrier V_{BASS} of the ^{54}Cr + ^{209}Bi reaction system was calculated by using the BASS nuclear-nuclear interaction potential [31].

IV. CONCLUSION

^{261,262}Bh have been studied and reinvestigated by using the fusion evaporation reaction ^{54}Cr + ^{209}Bi at the gas-filled recoil separator SHANS2. ^{262}Bh exhibits two distinct states with half-lives of 96^{+18}_{-13} and 21^{+8}_{-5} ms, respectively, and the half-life of ^{261}Bh was measured to be $8.9^{+2.2}_{-1.5}$ ms. At the beam energy of 264.1 MeV, the production cross sections of ^{262}Bh and ^{261}Bh were measured to be 703^{+261}_{-246} and < 33 pb, respectively, while they were 56^{+76}_{-40} and 174^{+92}_{-77} pb at 270.4 MeV. The half-life and cross-section data obtained in this work are consistent with the results from prior experiments.

ACKNOWLEDGMENTS

We would like to express our thanks to the accelerator crew and the ion source group of CAFE2 for providing the stable ^{54}Cr beam, and also our gratitude to Dr. F. P. Heßberger for calculating the cross section by using the HIVAP code. This work was partially supported by the Guangdong Major Project of Basic and Applied Basic Research (Grant No. 2021B0301030006), the Strategic Priority Research Program of Chinese Academy of Sciences (Grant No. XDB34010000), the National Key R&D Program of China (Contract No. 2023YFA1606500), the National Natural Science Foundation of China (Grants No. U1932139, No. 12105328, No. 12035011, No. U2032135, and No. 11975279), the Youth Innovation Promotion Association CAS (Grants No. 2020409 and No. 2023439), the CAS Project for Young Scientists in Basic Research (Grant No. YSBR-002), the Gansu Key Project for Science and Technology (Grant No. 23ZDGA014), and the Special Research Assistant Project of the Chinese Academy of Sciences.

[1] Y. T. Oganessian, A. Sobiczewski, and G. M. Ter-Akopian, Superheavy nuclei: from predictions to discovery, Phys. Scr. **92**, 023003 (2017).

[2] N. Bohr and J. A. Wheeler, The mechanism of nuclear fission, Phys. Rev. **56**, 426 (1939).

[3] Y. T. Oganessian and V. K. Utyonkov, Super-heavy element research, Rep. Prog. Phys. **78**, 036301 (2015).

[4] Y. T. Oganessian, A. G. Demin, N. A. Danilov, G. N. Flerov, M. P. Ivanov, A. S. Iljinov, N. N. Kolesnikov, B. N. Markov, V. M. Plotko, and S. P. Tretyakova, On spontaneous fission of neutron-deficient isotopes of elements 103, 105, and 107, Nucl. Phys. A **273**, 505 (1976).

[5] G. Münzenberg, S. Hofmann, F. P. Heßberger, W. Reisdorf, K. H. Schmidt, J. H. R. Schneider, P. Armbruster, C. C. Sahm, and B. Thuma, Identification of element 107 by α correlation chains, Eur. Phys. J. A **300**, 107 (1981).

[6] G. Münzenberg, P. Armbruster, S. Hofmann, F. P. Heßberger, H. Folger, J. G. Keller, V. Ninov, K. Poppensieker, A. B. Quint, W. Reisdorf, K.-H. Schmidt, J. R. H. Schneider, H.-J. Schött, K. Sümmerer, I. Zychor, M. E. Leino, D. Ackermann, U. Gollerthan, E. Hanelt, W. Morawek *et al.*, Element 107, Z. Phys. A **333**, 163 (1989).

[7] Commission on Nomenclature of Inorganic Chemistry, Names and symbols of transfermium elements (IUPAC recommendations 1997), Pure Appl. Chem. **69**, 2471 (1997).

[8] R. Eichler, W. Brüchle, R. Dressler, C. E. Düllmann, B. Eichler, H. W. Gäggeler, K. E. Gregorich, D. C. Hofman, S. Hübener, D. T. Jost, U. W. Kirbach, C. A. Laue, V. M. Lavanchy, H. Nitsche, J. B. Patin, D. Piguet, M. Schädel, D. A. Shaughnessy, D. A. Strellis, S. Taut *et al.*, Chemical characterization of bohrium (element 107), Nature (London) **407**, 63 (2000).

[9] S. L. Nelson, K. E. Gregorich, I. Dragojević, M. A. Garcia, J. M. Gates, R. Sudowe, and H. Nitsche, Lightest isotope of Bh produced via the ^{209}Bi(^{52}Cr, n) ^{260}Bh reaction, Phys. Rev. Lett. **100**, 022501 (2008).

[10] F. P. Heßberger, S. Antalic, D. Ackermann, S. Heinz, S. Hofmann, J. Khuyagbaatar, B. Kindler, I. Kojouharov, B. Lommel, and R. Mann, Alpha-decay properties of ^{261}Bh, Eur. Phys. J. A **43**, 175 (2010).

[11] S. Hofmann, V. Ninov, F. P. Hessberger, P. Armbruster, H. Folger, G. Münzenberg, H. J. Schött, A. G. Popeko, A. V. Yeremin, A. N. Andreyev, S. Saro, R. Janik, and M. Leino, The new element 111, Eur. Phys. J. A **350**, 281 (1995).

[12] Z. G. Gan, J. S. Guo, X. L. Wu, Z. Qin, H. M. Fan, X. G. Lei, H. Y. Liu, B. Guo, H. G. Xu, R. F. Chen, C. F. Dong, F. M. Zhang, H. L. Wang, C. Y. Xie, Z. Q. Feng, Y. Zhen, L. T. Song, P. Luo, H. S. Xu, G. M. Zhou *et al.*, New isotope ^{265}Bh, Eur. Phys. J. A **20**, 385 (2004).

[13] P. A. Wilk, K. E. Gregorich, A. Türler, C. A. Laue, R. Eichler, V. Ninov, J. L. Adams, U. W. Kirbach, M. R. Lane, D. M. Lee, J. B. Patin, D. A. Shaughnessy, D. A. Strellis, H. Nitsche, and D. C. Hoffman, Evidence for new isotopes of element 107: ^{266}Bh and ^{267}Bh, Phys. Rev. Lett. **85**, 2697 (2000).

[14] J. Khuyagbaatar, A. Yakushev, C. E. Düllmann, D. Ackermann, L.-L. Andersson, M. Asai, M. Block, R. A. Boll, H. Brand, D. M. Cox, M. Dasgupta, X. Derkx, A. Di Nitto, K. Eberhardt, J. Even, M. Evers, C. Fahlander, U. Forsberg, J. M. Gates, N. Gharibyan *et al.*, Fusion reaction ^{48}Ca + ^{249}Bk leading to formation of the element Ts ($Z = 117$), Phys. Rev. C **99**, 054306 (2019).

[15] Y. T. Oganessian, V. K. Utyonkov, N. D. Kovrizhnykh, F. S. Abdullin, S. N. Dmitriev, A. A. Dzhioev, D. Ibadullayev, M. G. Itkis, A. V. Karpov, D. A. Kuznetsov, O. V. Petrushkin, A. V. Podshibiakin, A. N. Polyakov, A. G. Popeko, I. S. Rogov, R. N. Sagaidak, L. Schlattauer, V. D. Shubin, M. V. Shumeiko, D. I. Solovyev *et al.*, New isotope ^{286}Mc produced in the ^{243}Am + ^{48}Ca reaction, Phys. Rev. C **106**, 064306 (2022).

[16] C. M. Folden III, S. L. Nelson, C. E. Düllmann, J. M. Schwantes, R. Sudowe, P. M. Zielinski, K. E. Gregorich, H. Nitsche, and D. C. Hoffman, Excitation function for the production of ^{262}Bh($Z = 107$) in the odd-Z-projectile reaction ^{208}Pb(^{55}Mn, n), Phys. Rev. C **73**, 014611 (2006).

[17] B. Štreicher, Synthesis and spectroscopic properties of transfermium isotopes with Z = 105, 106 and 107, Ph.D. thesis, Comenius University, Bratislava, Slovakia, 2006.

[18] S. L. Nelson, C. M. Folden III, K. E. Gregorich, I. Dragojević, C. E. Düllmann, R. Eichler, M. A. Garcia, J. M. Gates, R. Sudowe, and H. Nitsche, Comparison of complementary reactions for the production of ^{261,262}Bh, Phys. Rev. C **78**, 024606 (2008).

[19] F. P. Heßberger, S. Hofmann, B. Streicher, B. Sulignano, S. Antalic, D. Ackermann, S. Heinz, B. Kindler, I. Kojouharov, P. Kuusiniemi, B. Leino, M. Lommel, R. Mann, A. G. Popeko, Š. Šáro, J. Uusitalo, and A. V. Yeremin, Decay properties of neutron-deficient isotopes of elements from Z = 101 to Z = 108, Eur. Phys. J. A **41**, 145 (2009).

[20] L. N. Sheng, Q. Hu, H. Jia, Z. Y. Zhang, Z. Chai, B. Zhao, Y. Zhang, Z. G. Gan, Y. He, and J. C. Yang, Ion-optical design and multiparticle tracking in 3D magnetic field of the gas-filled recoil separator SHANS2 at CAFE2, Nucl. Instrum. Methods Phys. Res. Sect. A **1004**, 165348 (2021).

[21] S. Y. Xu, Z. Y. Zhang, Z. G. Gan, M. H. Huang, L. Ma, J. G. Wang, M. M. Zhang, H. B. Yang, C. L. Yang, Z. Zhao, X. Y. Huang, L. X. Chen, X. J. Wen, H. Zhou, H. Jia, L. N. Sheng, J. Q. Wu, X. L. Peng, Q. Hu, J. Yang *et al.*, A gas-filled recoil separator, SHANS2, at the China Accelerator Facility for Superheavy Elements, Nucl. Instrum. Methods Phys. Res. Sect. A **1050**, 168113 (2023).

[22] V1724 and vx1724 user manual, http://www.caen.it.

[23] M. Vostinar, F. P. Heßberger, D. Ackermann, B. Andel, S. Antalic, M. Block, C. Droese, J. Even, S. Heinz, Z. Kalaninova, I. Kojouharov, M. Laatiaoui, A. K. Mistry, J. Piot, and H. Savajols, Alpha-gamma decay studies of ^{258}Db and its (grand)daughter nuclei ^{254}Lr and ^{250}Md, Eur. Phys. J. A **55**, 17 (2019).

[24] B. Singh, Nuclear data sheets for A=254, Nucl. Data Sheets **156**, 1 (2019).

[25] J. M. Gates, M. A. Garcia, K. E. Gregorich, C. E. Düllmann, I. Dragojević, J. Dvorak, R. Eichler, C. M. Folden, W. Loveland, S. L. Nelson, G. K. Pang, L. Stavsetra, R. Sudowe, A. Türler, and H. Nitsche, Synthesis of rutherfordium isotopes in the ^{238}U(^{26}Mg, xn) $^{264-x}$Rf reaction and study of their decay properties, Phys. Rev. C **77**, 034603 (2008).

[26] P. Reiter, T. L. Khoo, C. J. Lister, D. Seweryniak, I. Ahmad, M. Alcorta, M. P. Carpenter, J. A. Cizewski, C. N. Davids, G. Gervais, J. P. Greene, W. F. Henning, R. V. F. Janssens, T. Lauritsen, S. Siem, A. A. Sonzogni, D. Sullivan, J. Uusitalo, I. Wiedenhöver, N. Amzal *et al.*, Ground-state band and

deformation of the $Z = 102$ isotope ^{254}No, Phys. Rev. Lett. **82**, 509 (1999).

[27] F. P. Heßberger, S. Hofmann, D. Ackermann, V. Ninov, M. Leino, G. Münzenberg, S. Saro, A. Lavrentev, A. G. Popeko, A. V. Yeremin, and C. Stodel, Decay properties of neutron-deficient isotopes ^{256,257}Db, ^{255}Rf, ^{252,253}Lr, Eur. Phys. J. A **12**, 57 (2001).

[28] W. Reisdorf, Analysis of fissionability data at high excitation energies, Z. Phys. A **300**, 227 (1981).

[29] W. Reisdorf and M. Schädel, How well do we understand the synthesis of heavy elements by heavy-ion induced fusion? Z. Phys. A **343**, 47 (1992).

[30] M. Wang, W. Huang, F. G. Kondev, G. Audi, and S. Naimi, The AME 2020 atomic mass evaluation (II). Tables, graphs and references, Chin. Phys. C **45**, 030003 (2021).

[31] R. Bass, Nucleus-nucleus potential deduced from experimental fusion cross sections, Phys. Rev. Lett. **39**, 265 (1977).